

DCB TEST SIMULATION OF STITCHED CFRP LAMINATES USING INTERLAMINAR TENSION TEST RESULTS

Kozue Nakane*, Naoyuki Watanabe*, Yutaka Iwahori**

*Tokyo Metropolitan University, **Japan Aerospace Exploration Agency

Keywords: CFRP laminate, DCB, interlaminar tension

Abstract

A mechanical model for the delamination extension of stitched laminates and 3-D orthogonal interlocked fabric composites has been developed by using a 2-D finite element method to simulate the experimental results of their DCB tests. The model is determined from the result of interlaminar tension tests of the specimens that includes only one through-the-thickness yarn, and the fracture phenomena around the through-the-thickness thread, such as debonding from the in-plane layer, slack absorption, fiber bridging, and the pull-out of broken threads from the in-plane layers, are introduced to the analytical model of the through-the-thickness yarn. The present FEM model is applied to examples of certain stitched laminates and a 3-D composite, and the analyses indicate good agreement with the experimental results, including the load-displacement curve and Mode I strain energy release rate. Since the present model of FEM analysis can simulate the experimental results in the DCB test for the stitched laminates and the 3-D composite, it is concluded that this innovative method of the interlaminar tension test and FEM analysis has a possibility of predicting the result of a DCB test without actually executing the DCB test.

1 Introduction

Fiber-reinforced composite materials have many advantages and are frequently used in a wide variety of applications [1,2], although most of them are two-dimensional (2-D) laminated composites. Therefore, interlaminar delamination is the weakest failure mode in such materials. Various techniques have been introduced to enhance interlaminar strength, and the most effective ones employ three-dimensional (3-D) textile technologies [3,4] such as

braiding, weaving, knitting, or a stitching process. Several types of 3-D fabrics have been developed and provide unique characteristics. Among them, the orthogonal interlocked fabric composite provides a fiber architecture aimed at retaining in-plane performance while increasing interlaminar toughness by introducing only a small amount of through-the-thickness (z-) reinforcement [5]. It is important to investigate quantitatively the influence of the z-direction reinforcement on the material performances for the trade-off study between in-plane and interlaminar properties in the design of fabric composite structures.

Several experimental studies about interlaminar toughness have been done for 3-D composites [6-9]. The results of these studies indicated that the existence of z-fiber yarns enormously increased the interlaminar fracture toughness and made the fracture phenomena more complex than those in 2-D composites. It was known that the presence of z-fibers caused various kinds of fracture phenomena, and these phenomena increased the interlaminar fracture toughness of this material. The strain energy release rate and its scatter became larger as the volume fraction of z-fiber yarn became higher [9].

Moreover, one of authors has executed an experimental study about the interlaminar delamination toughness of stitched CFRP laminates [10]. From those studies, it was found that the interlaminar toughness of stitched CFRP laminates was sufficiently larger than that of unstitched laminates and the strain energy release rate became larger as the stitch density increases. However, the phenomena that cause such an increase in performance has not been understood completely.

On the other hand, few analyses have been carried out about the interlaminar fracture toughness of 3-D composites. Watanabe et al. have developed the model and carried out the

numerical analysis [11-14]. Major points of consideration in the analysis of Ref. 11 are as follows:

- 1) Debonding of through-the-thickness fiber bundle from the in-plane layers;
- 2) Absorbing its slack given in the manufacturing process;
- 3) Tensile fracture and fiber bridging after its fracture.

With this model, the quantitative character of delamination extension, such as the effect of through-the-thickness fiber simulation of delamination extension, was carried out for the common and new type of 3-D orthogonal interlocked fabric composites [12,13]. From these calculations, it is proved that this model can simulate the actual phenomenon of delamination extension very well and it is possible to estimate the actual value of interlaminar fracture toughness in 3-D composite.

In this paper, a mechanical model for the delamination extension of stitched laminates and 3-D orthogonal interlocked fabric composites has been developed by using 2-D finite element method to simulate experimental results of their DCB tests. The fracture phenomena around through-the-thickness thread, such as debonding from the in-plane layer, slack absorption, fiber bridging, and pull-out of the broken thread from the in-plane layers, are introduced to the analytical model of through-the-thickness yarn, and this model is determined from the result in the interlaminar tension test of the specimen including only one through-the-thickness yarn. The present FEM model is applied to some stitched laminates and the 3-D composite.

2 Outline of Experiments

Some of the authors executed the experimental study about the interlaminar delamination toughness of stitched CFRP laminates. In this section, the summary of the experiments is given.

2.1 Material Systems and Specimen Configuration

The stitched CFRP laminates consisted of 24-ply quasi-isotropic $[45^\circ/0^\circ/-45^\circ/90^\circ]_{3S}$ fabric of T700-12K and they were stitched with Kevlar 29 yarn. As for the stitch thread, 800-d and 1200-d yarns were utilized and laminates were fabricated by changing a stitch space and stitch pitch. To consolidate the composite, the resin transfer

molding(RTM) technique was adopted, and its resin was TR-A31.

Figure 1 shows the specimen configuration and dimensions, which have been developed by Ishikawa *et al.* [8]. The unidirectional CFRP tabs that were 2.0 mm in thickness were bonded on both sides of the specimen. A cut-out, for inserting steel loading tongues that are useful when crack opening load becomes high, was machined into the specimen. An initial crack was given into this specimen with a very sharp razor. Stitch spacing is the distance between two adjacent stitch lines and stitch density is the number of stitch yarn per unit area. Since stitched yarns are running in the longitudinal direction of DCB specimens, stitch yarns are continuous in the longitudinal direction, that is, the delamination extension direction.

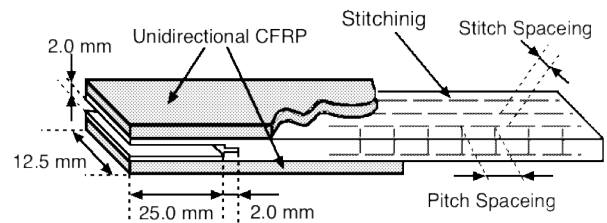


Figure 1 Configuration and Dimensions of DCB Test Specimen.

2.2 Procedure of DCB Tests

The DCB specimen was tested with the INSTRON 5500R screw-driven testing machine under a displacement-controlled mode with 0.25 mm/min or 0.50 mm/min crosshead speed. Figure 2 illustrates the schematic load-deflection curve for the present stitched laminates. The specimen was loaded till the load dropped suddenly at point A, and then the machine was stopped to measure the crack length. This procedure was repeated at each load drop. The curve of load versus crack opening displacement, which is assumed to be identical with its crosshead displacement, was plotted during the experiment with records of crack lengths. After the experiment, loads and opening displacements at moments when the load suddenly dropped were picked up. By using these data sets of load, displacement, and crack length, G_I was calculated by the area method, which is based on energy consideration suitable for the stitched composites. Let us consider the change from A to C, then G_I was calculated from the following expression :

$$G_I = \frac{1}{2b\Delta a} (P_1\delta_2 - P_2\delta_1) + \frac{1}{2b\Delta a} \Delta S \quad (1)$$

where ΔS , b , and Δa are the area of fan shaped region, the width of the specimen and crack growth length from point A to point C, respectively. The first load drop in one specimen was neglected because a dull initial artificial crack tip affects it.

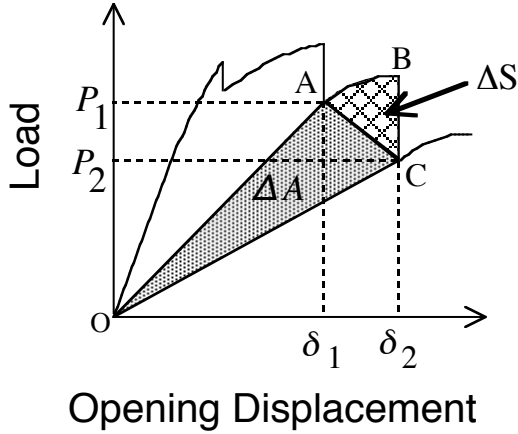


Figure 2 Schematic Load-Displacement Curve of 3-D Composite.

2.3 Procedure of Interlaminar Tension Tests

Figure 3 indicates the configuration and dimension of specimen for the interlaminar tension test. The specimen includes only one set of the upper and lower stitch threads at the center. It is bonded with test jigs on both the upper and lower surfaces, and it is subjected to the interlaminar tensile force. This test is continued until the stitch thread breaks and it is pulled out perfectly from the in-plane layers.

Figure 4 shows a typical result of the stitched laminate by Kevlar 1200d with a solid line. In these laminates, almost all specimens indicate nearly the same curve as shown in Fig. 4. On the other hand, curves of specimens with 800d are roughly classified into three types, although the results are not shown here for the lack of space.

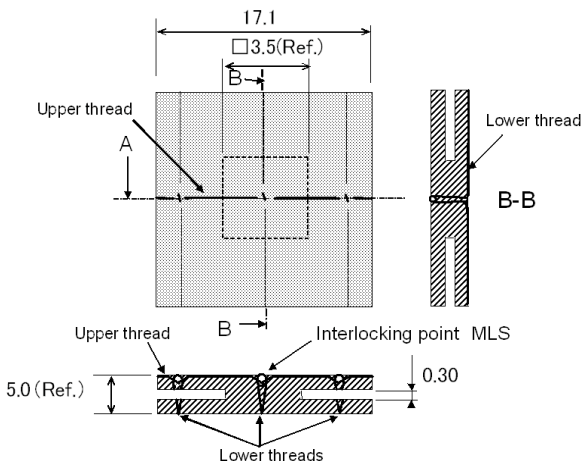


Figure 3 Configuration and Dimensions of Interlaminar Tension Test Specimen.

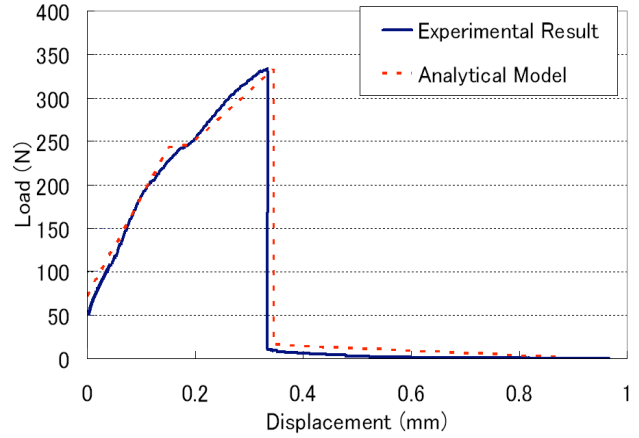


Figure 4 Load-Displacement Curve of Interlaminar Tension Test.

3 Modeling

The authors have developed a numerical model extracting the mechanical essence of interlaminar fracture toughness based on the experimental findings. To simplify the analysis, the crack front is assumed to be straight along the y -direction. Then, two-dimensional finite element analysis can be applied, and it was actually carried out under the plane stress condition. A delamination extension is evaluated by the Mode I strain energy release rate calculated by the crack closure technique [15]. The adhesive layer between the composite and unidirectional CFRP tab is neglected in modeling as shown in Fig. 5. In-plane layers of 0° , $\pm 45^\circ$, and 90° are homogenized into only one kind of orthotropic layer, and its equivalent elastic constants for are assumed to be as follows:

$$E_x = 62.17 \text{ GPa}$$

$$E_z = 7.40 \text{ GPa}$$

$$G_{xz} = 4.30 \text{ GPa}$$

$$\nu_{xz} = 0.38$$

where these constants are obtained experimentally by the tensile tests. And elastic constants of the unidirectional CFRP tab are assumed as follows:

$$E_x = 128.0 \text{ GPa}$$

$$E_z = 9.00 \text{ GPa}$$

$$G_{xz} = 4.37 \text{ GPa}$$

$$\nu_{xz} = 0.32.$$

Only one-half of the specimen is modeled, considering its symmetry. A typical finite element mesh for the tabbed DCB specimen is schematically shown in Fig. 5, where a_0 is an initial crack length measured from the loading point. An 8-noded rectangular element is employed to the in-plane layers and tabs. An element side length in the x -

direction is equal to the crack increment Δa employed in this study, where $\Delta a = 0.65$ mm. In addition, the effects of the loading fixture or steel loading tongues are modeled by an equivalent spring.

The behavior of the through-the-thickness fiber yarn in the 3-D orthogonal interlocked fabric composites during the crack extension has been modeled by authors [11,13], and the detailed explanation is given in Ref. 11. Hence, this model is adopted with a little modification. A typical mechanical process of through-the-thickness fiber yarn is schematically shown in Fig. 6. Some slack is introduced, considering manufacturing process. Unless the slack is introduced in the model, the z-fiber yarn may be broken as soon as or even before the crack tip reaches it. This presumption is completely contrary to the experimental observation, and the numerical prediction becomes far different from the actual behavior. Consequently, the idea of "slack" is very important and should be introduced in the present model. During the crack extension, the stitch thread debonds from the in-plane layers, and then the slack is absorbed, as shown in Fig. 6 (b) and (c). In the experiment, the stitch breakage after the debonding from the in-plane layer and the fiber bridging by a few or several broken stitch yarns were observed. Hence, these phenomena were modeled in the present analysis as illustrated in Fig. 6 (d) and (e). The frictional force between the stitch thread and in-plane layers is considered during its pullout. This force reduces the crack opening displacement and the released strain energy is consumed by it.

The fracture phenomena related to the stitch thread are simplified in the sequential manner in this model as follows:

1) The stitch thread is bonded perfectly at the beginning and debonds completely from the in-plane layers when its axial force reaches the designated limit load.

2) The absorption of slack occurs gradually until the total slack amounts to a certain ratio of its original length while its tensile load exceed the limit load. The effect of slack is handled by using pseudo-force explained in Ref. 11 in detail.

3) After the total slack reaches the limit, the stitch thread breaks when the axial force exceeds its tensile strength.

4) After breakage, it is pulled out until a relative displacement between the stitch and in-plane layer reaches a pre-determined limit based on the observation of tested specimens. A frictional force acts between the stitch and in-plane layer while the

stitch bridges the crack surface. In the present model, an effect of the breakage of epoxy region around the stitch threads is included in the friction during its pull-out, because the epoxy failure is not easy to model in the present framework. This mixed behavior is simply referred as "stitch slip" in this study.

In our former analyses, there were some parameters such as the load of debonding, amount of slack, change of friction, and so on, which could not be directly determined only from the experimental results. A few series of parametric studies are indispensable to estimate them accurately. In the present paper, the stitch thread behavior is directly determined to be a certain model where there is no unknown parameter and no ambiguity only from the results in the interlaminar tension tests, which are carried out before the analysis.

The stitch thread is modeled as a 3-noded rod element with constant sectional area A_z , with only an axial stiffness and its support. An effective longitudinal modulus of an array of the z-fiber bundles across the width direction (y) must be evaluated as a material property of the rod elements.

The initial vertical displacement is applied at the point A in Fig. 5 and the strain energy release rate is calculated by extending the crack virtually. If the calculated value is smaller than the critical strain energy release rate of the in-plane layers $G_{ICin-plane}$ basically determined by the experimental results, the opening displacement is increased till the strain energy release rate becomes larger than the critical value. The experimental observation revealed that $G_{ICin-plane}$ was small at the beginning of the crack extension, and then falls into a certain band.

The value of $G_{ICin-plane}$ is defined as the values when the crack extends in the in-plane layer between the stitch thread and includes no effect of the stitch slip. The analysis is executed until the crack length reaches approximately 100mm from the initial crack tip, and then the relations between the opening displacement and applied load are obtained.

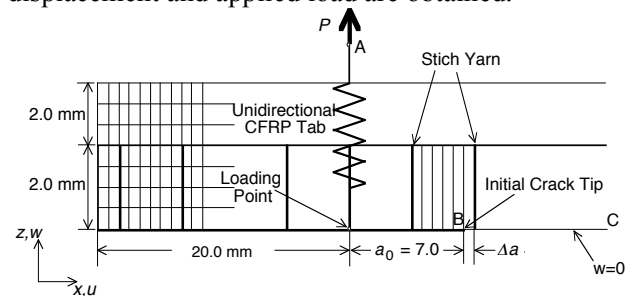


Figure 5 Finite Element Model of Tabbed DCB Test Specimen.

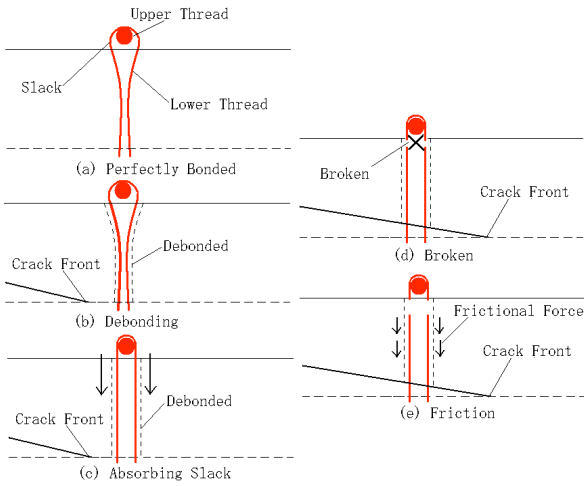


Figure 6 Model of Stitch Thread Behavior.

4 Numerical Results

4.1 Laminates without Stitching

In order to obtain the basic characteristic of delamination extension, the DCB test of the laminate without stitch thread was analyzed first. After some tuning, the analytical model without the stitch effect the numerical result was compared with the experiment. The comparison in the load-displacement curve is shown in Fig. 7. The experimental observation revealed that the $G_{ICin-plane}$ value was small at the beginning of the crack extension, and the fall into a certain band. Therefore, in this analytical model the initial value of $G_{ICin-plane}$ is 0.3 J/m^2 and it increases linearly to 0.6 J/m^2 when the crack length becomes 50 mm. Although the experimental curve shows a certain stick-slip behavior which does not appear in the analytical curve, the two curves are in good agreement with each other on the magnitude of peak load and decreasing trend of load after then.

To show the analysis ability in the other direction, numerical and experimental crack opening displacements are compared against the crack length in Fig. 8. It should be recalled that the experimental crack length was measured only from its load drops. The numerical values are very close to the averaged experimental curves, although there are some differences. Therefore, it is considered that the above estimation of $G_{ICin-plane}$ is reasonable.

The numerical G_I values in the laminate are obtained from the curves by the area method and compared with the experimental values as given in Fig. 9. The numerical result begins at 0.35 J/m^2 , and increases linearly to 0.6 J/m^2 at 50 mm crack length. This fact is natural because this is the input data of in-pane layers $G_{ICin-plane}$ value. In the experimental

result, there are some higher or lower values than the numerical ones, and it is indispensable fact in the experiment. If the averaged curve is drawn by a certain method from the experimental values, it is very close to the numerical result. From the comparison in the above three figures, it is indicated that our analytical model has a good ability to simulate the DCB test of the laminate without any stitching.

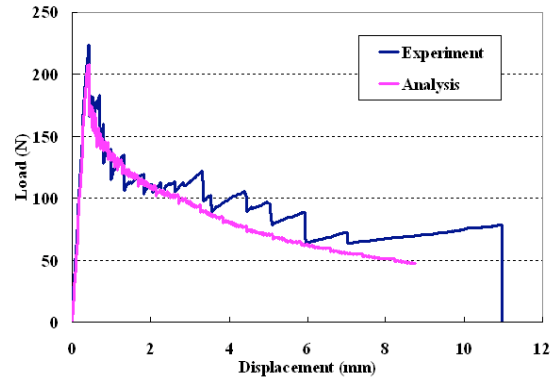


Figure 7 Comparative Load-Displacement Curve.

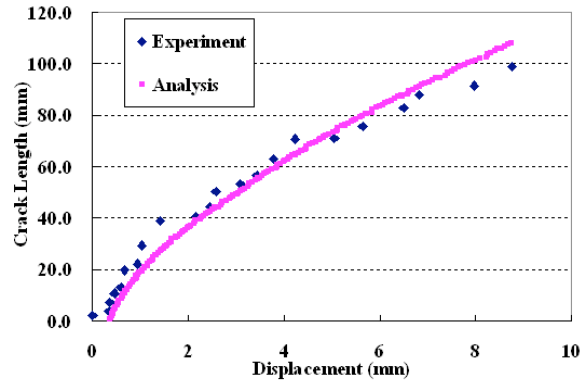


Figure 8 Crack Length as a Function of Crack Opening Displacement.

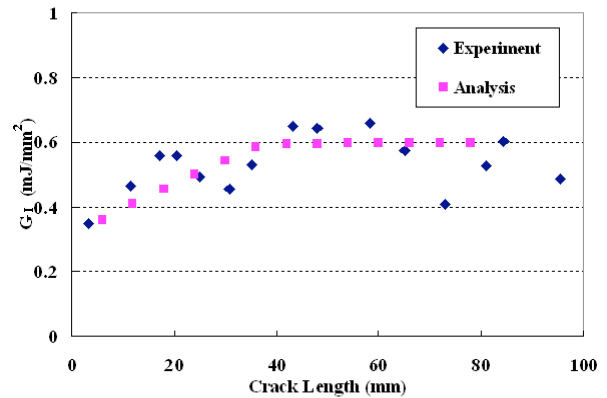


Figure 9 Strain Energy Release Rate as a Function of Crack Length.

4.2 Simulation of a Stitched Laminate with 1200d Kevlar

Figure 4 shows the load-displacement curve obtained in the interlaminar tension test and analytical model of the 1200d stitch thread. The amount of slack is assumed to be 1.0% of the original stitch length and it is introduced in the model, which is indicated as the constant load a little less than 250 N in Fig. 4. This stitch thread has only a very small frictional force during its pull out.

Figure 10 shows the load-displacement curves obtained by the experiments and analysis in the stitched laminate where the stitch space and stitch pitch are 9.0mm and 5.0mm, respectively. Although there are some difference in the magnitude of peak load and slightly early breakage of some stitch threads, the analytical curve is in a fairly good agreement with the experiment in the entire region.

Figure 11 shows a comparison on the Mode I strain energy release rate, G_I between the experimental results and numerical one, where G_I is obtained from the load-displacement curves in the both. The analytical value rises until the crack length reaches 60 mm, and after then it is nearly constant and its value is 3.40 mJ/mm². The distribution of the numerical result is in good agreement with the averaged experimental curve although there is a considerably large fluctuation in the experiment. The averaged analytical G_I is 2.98 mJ/mm² while the experimental one is 2.92 mJ/mm², and its difference is only 2.0%.

Figure 12 shows the Mode I strain energy release rate as a function of stitch density. It is clear that the relationship between G_I and stitch density is proportional in the both results, and then the approximate line can be drawn by the method of least squares. The line of the numerical result shows a good agreement with that of experiments. The value of its gradient by experiment is 122.2 while analytical one is 117.1, and its difference is only 4.2%. Because the stitch thread in this laminate with Kevlar 1200d stably breaks in type-B, the present FEM analysis can predict very accurately the results in the DCB test.

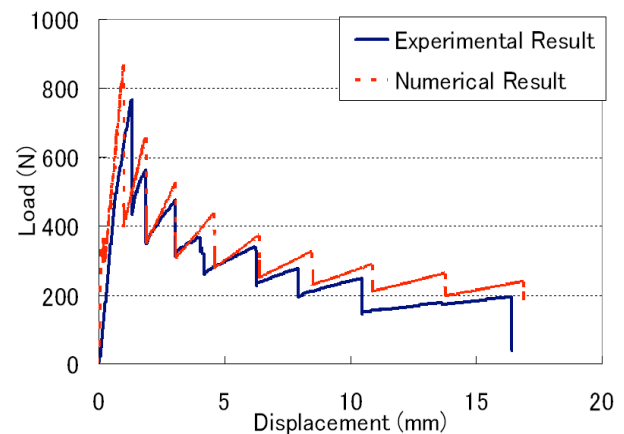


Figure 10 Load-Displacement Curve of DCB Test.

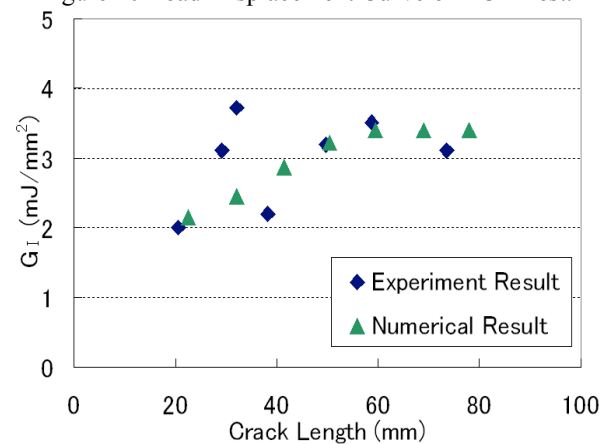


Figure 11 Strain Energy Release Rate as a Function of Crack Length.

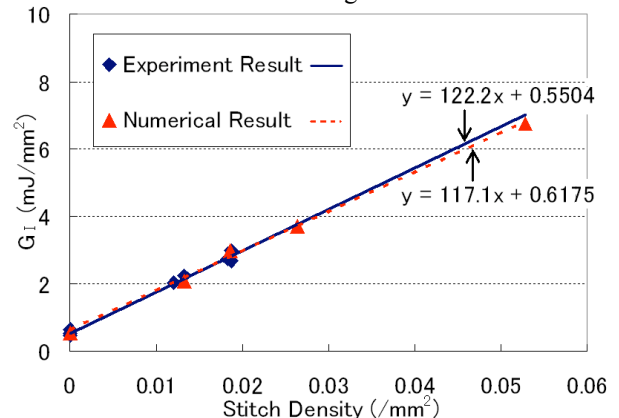


Figure 12 Strain Energy Release Rate as a Function of Stitch Density.

4.3 Simulation of a Stitched Laminate with 800d Kevlar

As for this laminate, three model types of the stitch tread are evaluated because the load-displacement curves in the interlaminar tension test are classified roughly into three types. These models are shown in Fig. 13. In type-A, the lower thread breaks near the upper thread like as shown in Fig. 6(d), and it is pulled out through a long distance

while the friction works. In type-B and -C, the lower thread breaks near the crack plane, and the friction is very small after then. From the observation in the DCB tests of this laminate, many type-B and a little type-A failure were observed. Therefore, models of type-A and B are adopted as the stitch mode in this laminate.

Figure 14 shows an experimental load-displacement curve and two numerical ones. In the small COD region, the experiment and two numerical curves are very similar to one another. In type-A the load becomes higher than the experiment when the COD exceeds 2.0 mm, since the number of bridging stitch threads increases and the frictional effect becomes very large. On the other hand, the curve of type-B becomes close to the experiment in the middle COD region. And the experiment curve becomes approaches the type-A curve in the large COD region. Therefore, the experimental state is considered to be like the type-B in the middle COD region and to approaches the type-A, since the mixture of type-A and -B failure was observed in the specimens after the DCB test.

Figure 15 shows both the experimental and numerical strain energy release rates as a function of the crack length. After the crack length exceeds 20 mm, most of the experimental values are close to ones in type-B analysis, but some values fairly larger than them, and moreover there is a value very close to the value of type-A analysis. From this fact it is confirmed that the experiment included both the stitch failure mode of type-A and B.

For this stitched laminate with Kevlar 800d, the numerical analysis is not able to accurately simulate the experiment, but it is considered that the analyses with both the type-A and B can give the upper and lower bounds to the experiment.

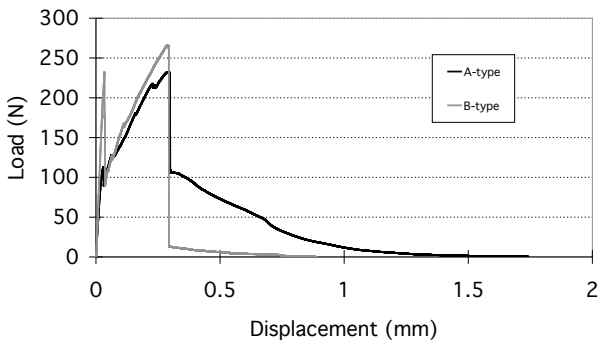


Figure 13 Load-Displacement Curve of Interlaminar Tension Test.

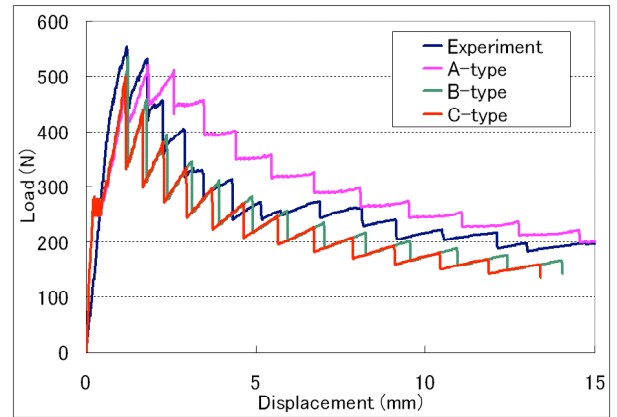


Figure 14 Load-Displacement Curve of FEM Analysis (Kevlar 800d).

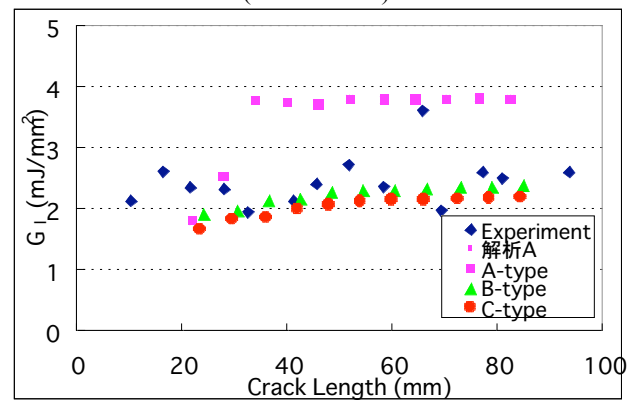


Figure 15 Crack Length and G_1 of FEM analysis (Kevlar-800d).

4.4 3-D Orthogonal Interlocked Fabric Composite

In this section, the result in the 3-D orthogonal interlocked fabric composite is mentioned, because this composite was fabricated in a similar manner to the stitching process. This fiber architecture is schematically illustrated in Fig. 16 and this was manufactured in Toyoda Automatic Loom Works, Ltd. In the in-plane layers and z-fiber yarn T-300 and T-900 are utilized, respectively. The resin is Epoxy#828 and the composite were made with the resin transfer molding (RTM) technique. The z-fiber tows are 2K, and its volume fraction is 0.5% including the portion of selvage yarn.

Figure 17 shows the experimental result in the interlaminar tension test and the model curve of z-yarn adopted in the FEM analysis. The peak load of z-yarn breakage or earlier behavior are not fairly different in comparison with the stitch threads, but the frictional force is very large and remains a high value during a long pull out of z-yarn. The friction at z-fiber break is 1.5 hold of that in 800d type-A model, which is the highest among the stitched laminates, and the displacement when the friction

disappears is larger than 3.0mm. It is known that the z-yarn of this 3-D composite can consume very much energy when it is tested in the DCB test [14]. The analytical model for z-yarn of this 3-D composite is determined as shown in Fig. 17.

The comparison on the load-displacement curves between the analysis and experiment is shown in Fig. 18. For the both results, the load increases almost linearly, then drops abruptly when the crack extends. The crack extends step by step unstably, and it is not smooth. The load drops every time the crack extends, and the amount of the load drop is independent of the opening displacement. The peak load decreases gradually as the crack extension. Therefore, the analysis can simulate the experimental curve fairly well although there are some differences in the detail of the middle COD region and the analytical curve is slightly higher in the large COD region.

Figure 19 shows a comparison of Mode I strain energy release rate G_I between the experiment and analysis as a function of the crack length. There are a few very high or very low values in the experiment because of the ambiguity in determining a crack extension length. Both of the curves begin at a value a little smaller than 5.0 J/m^2 , they rise to approximately 15.0 J/m^2 at 20 mm crack length, and then they remain nearly constant at a value a little smaller than 15.0 J/m^2 . The numerical averaged value of G_{IC} is 13.06 J/m^2 and shows good agreement with the experimental G_{IC} value of 12.75 J/m^2 .

Figure 20 indicates the photograph of the crack surface in the tested DCB specimen of this 3-D composite. Almost all of z-yarn breaks in type-A and they are pulled out in nearly the same shape as the original shape before the test. It is considered that this failure mechanism of z-yarn leads to the very high toughness characteristic. Because the z-fiber yarn in this 3-D composite stably breaks in type-A, the present FEM analysis can predict very accurately the results in the DCB test.

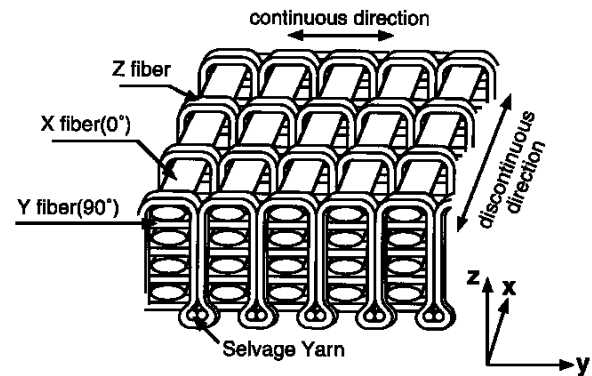


Figure 16 Fiber Architecture of 3-D Composite.

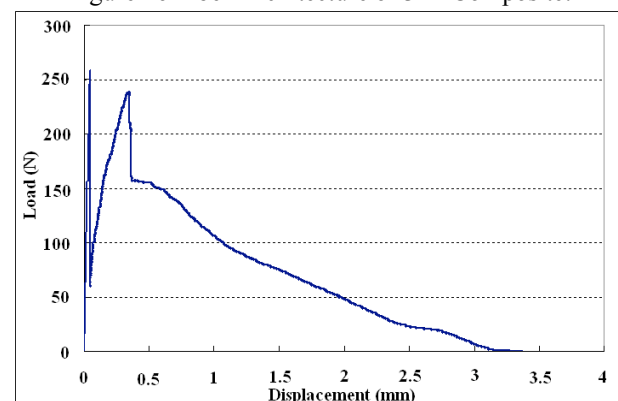


Figure 17

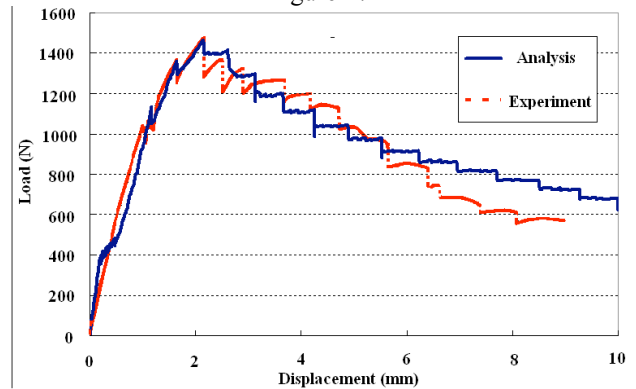


Figure 18 Load-Displacement Curve of 3-D Composite.

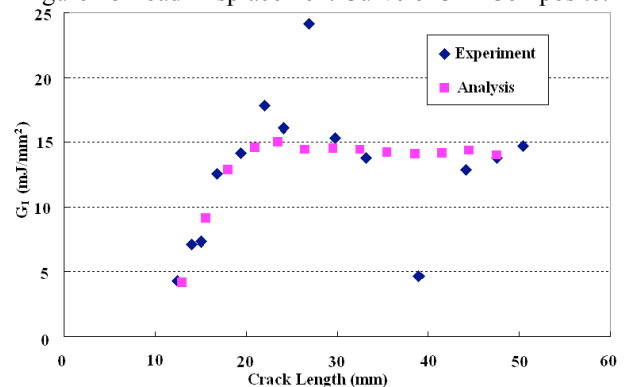


Figure 19 Strain Energy Release Rate as a Function of Crack Length.

5 Conclusion

A mechanical model for the delamination extension of stitched laminates and 3-D orthogonal interlocked fabric composites has been developed by using 2-D finite element method to simulate experimental results of their DCB tests. The fracture phenomena around the through-the-thickness thread, such as debonding from the in-plane layer, slack absorption, fiber bridging, and pull-out of a broken thread from the in-plane layers, are introduced to the analytical model of through-the-thickness yarn. This model is determined from the result of the interlaminar tension test of a specimen that includes only one through-the-thickness yarn. The present FEM model is applied to some stitched laminates and 3-D composite. The conclusions are obtained as follows:

1. The mechanical model, which is determined from the load-displacement curve of the interlaminar tension test, indicated the complicated behavior of the through-the thickness thread in the DCB test fairly well.
2. As for the stitched laminate with Kevlar-29 1200d thread and 3-D orthogonal interlocked fabric composite, the present FEM simulation predicted the experimental results including the load-displacement curves and Mode I strain energy release rates very accurately, because almost all of the through-the thickness threads in the DCB test broke in the same way as that in the interlaminar tension test.
3. Since stitch threads in the DCB test broke in two ways randomly for the stitched laminates with Kevlar-29 800d thread, the present simulation could not predict an accurate behavior. But the present method could give the upper and lower bounds of the result to such laminates by considering the broken way of stitch thread in the interlaminar tension test.
4. From the above results it is proved that this innovative method of the interlaminar tension test and FEM analysis has a possibility to predict the result of DCB tests without executing the actual DCB test.

Acknowledgements

The authors would like to thank the co-researchers of the Japan Aerospace Exploration Agency (JAXA), without whom the research could not have been carried out.

References

- [1] Mallick, P. K., “*Fiber-Reinforced Composite; materials, manufacturing, and design*”, 2nd ed., Marcel Dekker Inc., New York, 1993.
- [2] Whitney, J. M., “Experimental characterization of delamination fracture”, *Interlaminar Response of Composite Materials*, Composite Material Series 5, Pagano, N. J. Ed., Elsevier Science Publishers B.V., New York, 1989.
- [3] Ko, F. K., “Three-dimensional fabric for composite”, *Textile Structural Composite*, Chou, T. W. and Ko, F. K. Ed., Elsevier Publisher, New York, 1989.
- [4] Chou, T. W., “*Microstructural Design of Fiber Composites*”, Cambridge University Press, New York, 1992.
- [5] Guenon, V. A. F., Chou, T. W and Gillespie, J. W., “Toughness properties of a three-dimensional carbon-epoxy composite”, *Journal of Material Science*, **24** (1989) 4168-75.
- [6] Watanabe, N., Oshiba, S., Ishikawa, T., “In-plane mechanical properties of CF/Epoxy 3-D orthogonal interlocked fabric composite”, *Proceedings of International Conference Composite Materials*, Paris, France, 1999.
- [7] Ishikawa, T., H., Ji, M., Anahara, M. and Yasui, Y., “The estimation of fracture of orthogonal three-dimensional fiber-reinforced composite by DCB testing”, *Proceedings of 71st Annual General Meeting of the Japan Society of Mechanical Engineers*, Tokyo, Japan, 455-7, 1994. (in Japanese).
- [8] Ishikawa, T., Matsushima, M., Bansaku, K., Watanabe, N. and Sunakawa, M., “Experimental results of interlaminar fracture toughness and in-plane strength of 3-D woven carbon/epoxy plates”, *Proceedings of Seminar of the Japan Society for Composite Materials*, Tokyo, Japan (1996) 51-2. (in Japanese).
- [9] Tanzawa, Y., Watanabe, N. and Ishikawa, T., “Interlaminar fracture toughness of 3-D orthogonal interlocked fabric composite”, *Composite Science and Technology* **59** (1999) 1261-1270.
- [10] Iwahori, Y., Ishikawa, T., Hayashi, Y., and Watanabe, N., “Study of interlaminar fracture toughness improvement on stitched CFRP laminates”, *Journal of the Japan Society for Composites Materials*, **26** (2000) 90-100 (in Japanese).
- [11] Watanabe, N. and Tanzawa, Y., “Delamination analysis of 3-D orthogonal interlocked fabric composite”, *Proceedings of 37th AIAA SDM Conference*, Salt Lake City, U.S.A., 877-85, 1996.
- [12] Watanabe, N. and Tanzawa, Y. and Ishikawa, T., “FEM simulation of modified DCB test for 3-D orthogonal interlocked fabric composite”,

Proceedings of 40th AIAA SDM Conference, St. Louis, Missouri, U.S.A., AIAA-99-1246, 1999.

- [13] Tanzawa, Y., Watanabe, N. and Ishikawa, T., “FEM simulation of a Modified DCB test for 3-D orthogonal interlocked fabric composite”, *Composite Science and Technology* **61** (2001) 1097-1107.
- [14] Watanabe, N. and Nishii, N., “DCB test and analysis of new 3-D orthogonal interlocked fabric composite FEM simulation of modified DCB test for 3-D orthogonal interlocked fabric composite”, *Proceedings of 41st AIAA SDM Conference*, Atlanta, Georgia, U.S.A., 2000.
- [15] Rybicki, E. F. and Kanninen, M. F., “A finite element calculation of stress intensity factors by a modified crack closure integral”, *Engineering Fracture Mechanics*, **9** (1997) 931-8.